Final Report on Modeling a SOFC at Various Fuel Concentrations to Analyze Load-Following Capability

Lydia Meyer

December 2020

1 Introduction

For our semester project, Rachel and I have explored the transient response capabilities of solid oxide fuel cells (SOFCs), as a function of temperature and pressure. For several reasons, using SOFCs at grid scale is increasingly appealing. Given their characteristically high operating efficiency and fuel flexibility, SOFCs are uniquely suited to reduce greenhouse gas emissions, relative to traditional coal generation plants and natural gas turbine generators, due to methane leak during combustion and upstream leak during fracking and refinement. Furthermore, the high operating temperature allows for waste heat to be recuperated in a bottoming cycle or used directly as a byproduct in a combined power and heat generation plant. We modeled the nickel anode of a simple SOFC [3]. The fuel was assumed to be pure hydrogen which is supplied to the anode. The half-cell reactions of the anode and cathode, respectively, are as follows:

$$O_2 + H_2 \longrightarrow H_2O + 2e^- \tag{1}$$

$$O_2 + 4e^- \longrightarrow 2O^{2-} \tag{2}$$

The fuel cell has been modeled in Cartesian coordinates and resembled the one below.

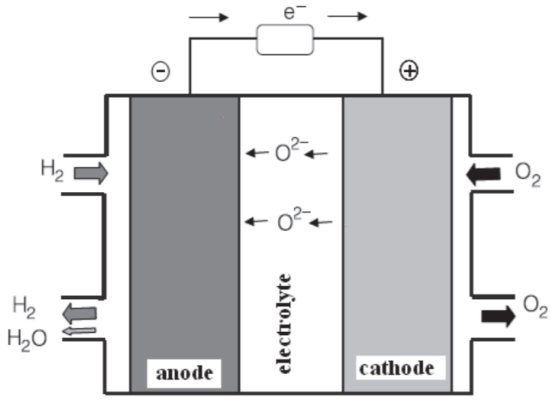

Figure 1: Fuel cell diagram [5]

The objective of this project was to expand upon the concepts taught in Electrochemical Systems and discover what parameters are important for optimizing the function a SOFC at various current demands.

2 Modeling Approach

The model utilized a focus on mass-action kinetics in an effort to zoom in on the intricacies of processes in the anode. The specifics of the governing equations and many of the initial values used in the model were inspired by the work of DeCaluwe et al. [2]. The following tables show the values used in the model.

Initial molar fractions	
Name	Value
Hydrogen in nickel	0.9
Vacancy in nickel	0.1
OH^+ in YSZ	0.4
O_2^- in YSZ	0.4
Vacancy in YSZ	0.1
H_2O in YSZ	0.1
O_2 in LSM	0.8
Vacancy in LSM	0.2

Species standard-state thermo at 800°		
Species	Enthalpy [J/kmol]	Entropy [J/kmol-K]
Hydrogen in nickel	-9.1e6	8.02e4
O_2^- in YSZ	-1.223e8	1.289e5
Vacancy in nickel	2e7	3.31e4
OH^+ in YSZ	4.78e7	1.66e5
H_2O in YSZ	-2.934e8	1.77e5

Mass-action kinetics were used to determine the potential drop across the anode, $\Delta\phi$, in various parametric studies. First, the Gibbs free energy for each species was determined, as well as the Gibbs free energy across the anode considering the temperature and species concentrations.

$$g_j = h_j - T * s_j \tag{3}$$

$$\Delta g^{\circ}_{anode} = \sum g_i - \sum g_j \tag{4}$$

$$\Delta g_{anode} = \Delta g^{\circ}_{anode} + RT \log(C) \tag{5}$$

where C is the normalized volume fraction of species in the anode. The forward and reverse reaction rate coefficients were also determined.

$$k^*_{fwd} = A_{fwd} \exp \frac{-E_{act}}{RT} \tag{6}$$

$$k_{fwd} = k^*_{fwd} \exp \left[\frac{-\alpha_{fwd} n F \Delta\phi}{RT} \right] \tag{7}$$

$$k_{rev} = k_{fwd} \exp \left[\frac{\Delta g_{anode} + nF\Delta\phi}{RT} \right] \tag{8}$$

where α_{fwd} is the anodic transfer coefficient and n is the charge equivalent transferred in the anode. The heat transfer due to reaction was also determined by the model

$$\dot{q}_1 = \gamma^2_{surf} \left(k_{fwd} X_{H^+} X_{O_2^-} - k_{rev} X_{Ni} X_{OH^-} \right) \tag{9}$$

$$\dot{q}_2 = \gamma^2_{surf} \left(k_{fwd} X_{H^+} X_{OH^-} - k_{rev} X_{H_2O} X_{OH^-} \right) \tag{10}$$

where X_{H^+} is the volume fraction of hydrogen ions in the nickel, $X_{O_2^-}$ is the volume fraction of oxygen ions in the YSZ, X_{Ni} is volume fraction of vacancies in the nickel, X_{OH^+} is the volume fraction of hydroxides in the YSZ, X_{H_2O} is the volume fraction of water in the YSZ, and γ_{surf} is the preexponential coefficient. The model also determined the Faradaic current in the anode

$$i_{Far} = nF\left(\dot{q}_1 + \dot{q}_2\right) \tag{11}$$

and the double-layer current

$$i_{dl} = i_{ext} - i_{Far} \tag{12}$$

where i_{ext} is the current demand placed upon the SOFC. Finally, the anode potential was determined by the following equation

$$\frac{dSV}{dt} = \frac{-i_{dl}}{C_{dl}} \tag{13}$$

where $\frac{dSV}{dt}$ is the change in the state variable at each time step, and C_{dl} is the double-layer capacity of the anode.

3 Results and Conclusion

The model worked somewhat well. Many values were chosen without a wealth of background knowledge on the subject, so they could have contributed to the model's shortcomings, such as the need for a large capacity for the model to solve the initial value problem. The model was able to solve in a short amount of time, though some of the results seem problematic. First, the polarization curve required a large current in order for it to resolve, which makes sense based on the large capacity.

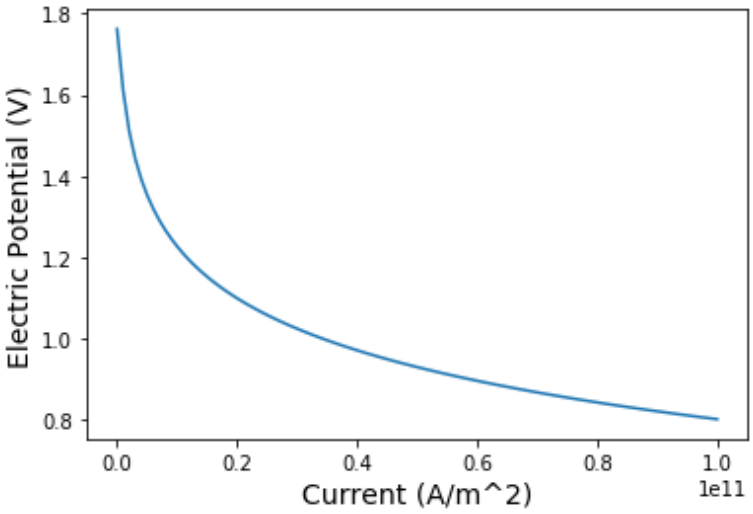

Figure 2: Polarization Curve

The SOFC model resolved to a potential of about 0.8V. In an experiment with identical SOFC anode chemistry and at the same temperature, Yoon et al. reached a potential of 0.2 V with a much lower current density, so it is clear that some parameters of this model are off [6]. The need for the large capacity value seems to stem from the calculation of large i_{Far} values, which are most likely due to incorrect initial potentials and concentration values.

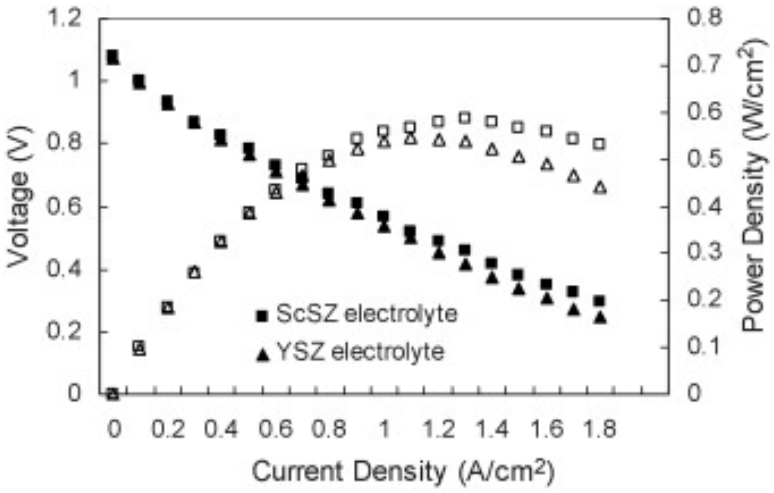

Figure 3: Experimental polarization curve [6]

Because of the large current required to drive the anode to steady state, we were not able to demonstrate its load following capabilities by varying the current. If, in reality, a cell had a capacity the size of this one, it should not be used for a scenario in which rapid ramping up and down would be required. This would be better for powering any stationary large equipment over long periods of time.

The concentrations of vacancies and hydrogen molecules were also varied to observe the effect on the anode potential.

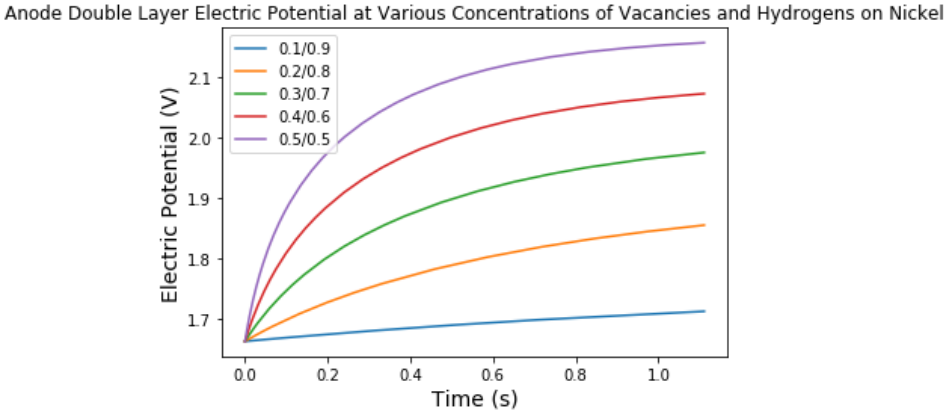

Figure 4: Potential dependence on i_{ext}

Interestingly, when the concentration of vacancies and hydrogen was identical, the cell had the greatest potential. Based on equations 10-13, this makes sense because a large concentration of vacancies will increase i_{Far} and decrease i_{dl}, which will result in a larger potential. In an experimental study of a SOFC fuel cell doped with H_2S, Lee et al. found that the cell voltage dropped when more fuel was supplied as a result of surface deposition without adequate removal [4].

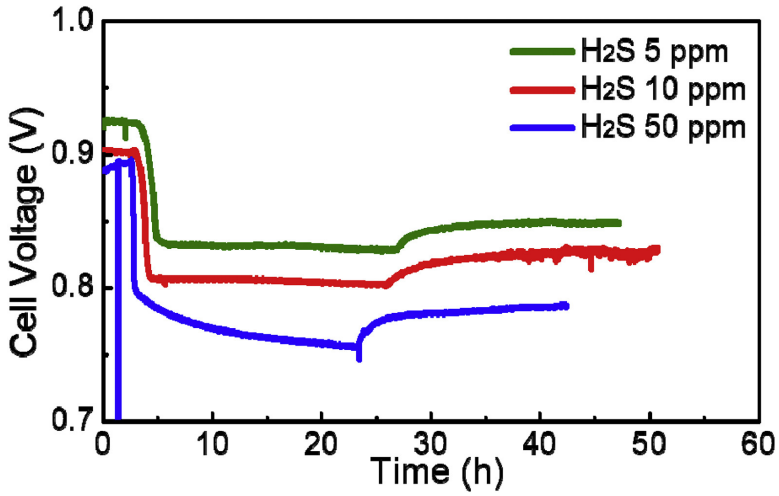

Figure 5: Impact of fuel increase on potential [4]

Though it seems unlikely that this model is complex enough to capture that possible dynamic, it is interesting that the results were similar.

4 Conclusion

Though this model was a decent foundation for a more complete SOFC model, it does leave much to be desired. First, the transport capabilities were not integrated with the charge transfer model, and with more time to make additions, that capability would be added first. Also, a cathode model was originally part of the model but did not behave well and was removed. The cathode would also be interesting to add to see the exchange of charge between the anode and cathode. Another interesting study would be to change the fuel coming in to be syngas and not pure hydrogen in the interest of better understanding this SOFC's situational flexibility. This has been studied experimentally by Campitelli et al., who found that the performance of the SOFC with biomass depends significantly on airflow and thermal considerations of the fuel cell [1]. Important future research should include the study of very specific biomass, particularly with mixtures abundant in certain rural areas of the world where biomass is readily available but where grid connectivity is either too challenging to pursue or too expensive. Fuel cells, in general, represent an important opportunity for further energy equity, though models like this one must be used to ensure successful deployment.

References

[1] Gennaro Campitelli, Stefano Cordiner, Mridul Gautam, Alessandro Mariani, and Vincenzo Mulone. Biomass fueling of a SOFC by integrated gasifier: Study of the effect of operating conditions on system performance. *International Journal of Hydrogen Energy*, 38(1):320–327, January 2013.

[2] Steven C. DeCaluwe, Peter J. Weddle, Huayang Zhu, Andrew M. Colclasure, Wolfgang G. Bessler, Gregory S. Jackson, and Robert J. Kee. On the Fundamental and Practical Aspects of Modeling Complex Electrochemical Kinetics and Transport. *Journal of the Electrochemical Society*, 165(13):E637, September 2018. Publisher: IOP Publishing.

[3] Thomas Francis Fuller and John Naim Harb. *Electrochemical engineering*. Wiley, Hoboken, NJ, USA, first edition edition, 2018.

[4] Ho Seong Lee, Hyun Mi Lee, Jun-Young Park, and Hyung-Tae Lim. Degradation behavior of Ni-YSZ anode-supported solid oxide fuel cell (SOFC) as a function of H2S concentration. *International Journal of Hydrogen Energy*, 43(49):22511–22518, December 2018.

[5] Jacqueline Santos and Tulio Matencio. Ceramic Materials for Solid Oxide Fuel Cells. August 2011.

[6] Kyung Joong Yoon, Peter Zink, Srikanth Gopalan, and Uday B. Pal. Polarization measurements on single-step co-fired solid oxide fuel cells (SOFCs). *Journal of Power Sources*, 172(1):39–49, October 2007.